第 35 卷第 12 期
2019 年 12 月

无 机 化 学 学 报
CHINESE JOURNAL OF INORGANIC CHEMISTRY

Vol.35 No.12
2355-2363

基于柠康酸构筑的三个配合物的合成、结构与性能

李桂连[1] 尹卫东[2] 刘乾龙[1] 李晓玲[1] 辛凌云[1] 刘广臻*,[1]

([1]洛阳师范学院化学化工学院,洛阳 471934)

([2]洛阳师范学院食品与药品学院,洛阳 471934)

摘要：在水热条件下,制备出 3 个配位聚合物,即{[Zn(ca)(iimb)]·0.75H_2O}$_n$ (**1**),{[Cd(ca)(iimb)(H_2O)]·0.75H_2O}$_n$ (**2**)和{[Zn(ca)(bpe)$_{0.5}$(H_2O)]·H_2O}$_n$ (**3**)(H_2ca=柠康酸,iimb=1-(1-咪唑基)-4-(咪唑基-1′-甲基)苯,bpe=1,2-二(4-吡啶基)乙烯),并通过单晶 X 射线衍射、红外光谱和元素分析进行结构表征。配合物 **1** 是含有一维金属羧酸链的二维网状层。**2** 是具有羧酸桥连双核的一维准梯形链状结构。**3** 是二维波浪层。其中 **2** 和 **3** 的三维超分子结构由丰富的氢键相互作用形成;而 **1** 的三维超分子结构通过范德华力堆积而成。研究了 3 个配合物的热重分析(TGA),粉末 X 射线衍射(PXRD)和荧光性质。固态荧光光谱表明 3 个配合物的发射光谱与相应的辅助配体相似。此外,配合物 **3** 在紫外光照射下,在 H_2O_2 存在时对亚甲基蓝(MB)的降解表现出良好的光催化活性。

关键词：柠康酸；水热合成；荧光性质；光催化降解

中图分类号：O614.24+1；O614.24+2 **文献标识码**：A **文章编号**：1001-4861(2019)12-2355-09

DOI：10.11862/CJIC.2019.271

Syntheses, Structures and Properties of Three Coordination Polymers Based on Citraconic Acid

LI Gui-Lian[1] YIN Wei-Dong[2] LIU Qian-Long[1] LI Xiao-Ling[1] XIN Ling-Yun[1] LIU Guang-Zhen*,[1]

([1]*College of Chemistry and Chemical Engineering, Luoyang Normal University, Luoyang, Henan* 471934, *China*)

([2]*School of Food and Drug, Luoyang Normal University, Luoyang, Henan* 471934, *China*)

Abstract: Three coordination polymers, {[Zn(ca)(iimb)]·0.75H_2O}$_n$ (**1**), {[Cd(ca)(iimb)(H_2O)]·0.75H_2O}$_n$ (**2**) and {[Zn(ca)(bpe)$_{0.5}$(H_2O)]·H_2O}$_n$ (**3**) (H_2ca=citraconic acid, iimb=1-(1-imidazolyl)-4-(imidazol-1-ylmethyl)benzene, bpe=1,2-di(4-pyridyl)ethylene), were synthesized hydrothermally and measured structurally by single crystal X-ray diffraction, infrared spectroscopy (IR) and elemental analysis. Complex **1** displays a 2D reticular layer containing 1D metal-carboxylate chains. **2** features a 1D quasi-trapezoidal shape chain structure containing carboxylate-bridged dinuclear structures. Complex **3** shows a two-dimensional wave layer. The three-dimensional supramolecular structures of **2** and **3** are formed by abundant H-bond interactions; nevertheless, 3D supramolecular structure of **1** is formed through weak van der Waals force. Thermogravimetric analyses (TGA), powder X-ray diffractions (PXRD) and fluorescence properties for complexes **1**~**3** were investigated. The solid state fluorescence spectra indicate that all emission spectra of three complexes **1**~**3** are similar with those of the corresponding auxiliary ligands. In addition, complex **3** exhibits good photocatalytic activity for methylene blue (MB) degradation in the presence of H_2O_2 under UV irradiation. CCDC: 1913976, **1**; 1913977, **2**; 1913978, **3**.

Keywords: citraconic acid; hydrothermal synthesis; fluorescence property; photocatalytic degradation

收稿日期:2019-05-28。收修改稿日期:2019-09-12。

国家自然科学基金(No.21571092)和河南省高等学校重点科研项目计划(No.18B150016)资助。

*通信联系人。E-mail:gzliuly@126.com

In recent years, the development of transition metal coordination polymers has been more oriented towards the development of practical applications, such as gas storage/separation, magnetism, catalysis and luminescent sensing[1-7]. The suitable ligands are the key to the design and synthesis of transition metal coordination polymers with interesting structures and good application performances. In the O-donor ligands, the aliphatic carboxylates are widely used in making diverse transition metal coordination polymers due to good flexibility and diverse coordination modes[8]. In our previous work, we obtained a number of transition metal coordination polymers with the fascinating structures and excellent properties based on a flexible itaconic acid[9-10]. The citraconic acid is an isomer of itaconic acid; they are very cheap and excellent flexible ligands with diverse coordination modes. However, there are still few reports on the synthesis of transition metal complexes by citraconic acid as a ligand[11-12].

The N-donor ligands are often used to mediate the structures and properties of transition metal coordination polymers together with the carboxylate groups[13-14]. In the N-donor ligands, 1,2-bi(4-pyridyl) ethylene (bpe) is one of the most common auxiliary ligands to combine with carboxylates main ligands to obtain a series of transition metal complexes with different structures and properties[15-18]. But as far as we know, there is no report about the 1-(1-imidazolyl)-4-(imidazol-1-ylmethyl)benzene (iimb) as an auxiliary N-donor ligand together with polycarboxylates ligands to synthesize the transition metal coordination polymers until now. In this work, we used flexible citraconic acid (H_2ca) as a dicarboxylate ligand and two N-donor ligands such as iimb and bpe as synergistic ligands to synthesize three coordination polymers by hydrothermal techniques, namely $\{[Zn(ca)(iimb)]\cdot 0.75H_2O\}_n$ (**1**), $\{[Cd(ca)(iimb)(H_2O)]\cdot 0.75H_2O\}_n$ (**2**) and $\{[Zn(ca)(bpe)_{0.5}(H_2O)]\cdot H_2O\}_n$ (**3**). The structures of three complexes are characterized by elemental analysis, infrared spectroscopy and single crystal X-ray crystallography. The fluorescence properties, thermal stabilities and powder X-ray diffraction for three complexes are given in this paper. The photocatalytic activity of **3** is evaluated by degradation of methylene blue under UV light.

1 Experimental

1.1 Materials and methods

Citraconic acid and bpe were purchased from J&K Scientific Ltd. Ligand iimb was purchased from Jinan Henghua Technology Co., Ltd. All other chemical reagents were of analytical grade and obtained from Tianjin Deen Chemical Reagent Co., Ltd. All chemical reagents were used without further purification. Elemental analyses for C, H and N were performed on a Flash 2000 organic elemental analyzer. Infrared spectra (4 000~600 cm^{-1}) were recorded on powdered samples using a Nicolet 6700 FT-IR spectrometer. Powder X-ray diffraction (PXRD) patterns were taken on a Bruker D8-ADVANCE X-ray diffractometer with Cu $K\alpha$ radiation (λ=0.154 18 nm; generator voltage: 40 kV; generator current: 40 mA; scanning scope, 2θ: 5°~50°). Thermogravimetric analyses were carried out on a SⅡ EXStar 6000 TG/DTA6300 analyzer heated from 25 to 800 ℃ with a heating rate of 10 ℃·min^{-1} in N_2 atmosphere. Solid fluorescence spectra were performed on an Aminco Bowman Series 2 luminescence spectrometer at room temperature. Solid-state ultraviolet/visible (UV/Vis) diffuse-reflectance spectrum was measured employing a UV-Vis spectrophotometer (Shimadzu, UV-3600 Plus) and a $BaSO_4$ plate was used as the reflectance standard. Solution UV spectra were tested on a Hitachi U-3010 UV-Vis spectrophotometer in the 10 mm quartz cuvette.

1.2 Synthesis of $\{[Zn(ca)(iimb)]\cdot 0.75H_2O\}_n$ (1)

A starting mixture containing $Zn(OAc)_2\cdot 2H_2O$ (43.8 mg, 0.20 mmol), H_2ca (13.0 mg, 0.10 mmol), iimb (22.4 mg, 0.10 mmol) and H_2O (5 mL) was heated at 120 ℃ for 4 days under autogenous pressure in a 23 mL Teflon-lined autoclave, then cooled to room temperature. Colorless needle crystals of **1** were collected in 58% yield. Elemental analysis Calcd. for $C_{18}H_{17}N_4O_{4.75}Zn$(%): C, 50.19; H, 3.98; N, 13.01. Found(%): C, 49.69; H, 4.02; N, 12.85. Selected IR (KBr, cm^{-1}): 3 129(w), 1 588(s), 1 524(s), 1 437(m), 1 401(s), 1 252

(s), 1 102(s), 1 065(m), 1 031(m), 953(m), 864(m), 830 (m), 754(s), 654(m).

1.3 Synthesis of {[Cd(ca)(iimb)(H_2O)]·0.75H_2O}$_n$ (2)

A mixture of $Cd(OAc)_2·2H_2O$ (54.0 mg, 0.2 mmol), H_2ca (0.013 g, 0.10 mmol), iimb (22.4 mg, 0.10 mmol), NaOH (4.0 mg, 0.10 mmol) and 5 mL H_2O was heated at 120 ℃ for 4 days under autogenous pressure in a 23 mL Teflon-lined autoclave, then colorless needle crystals were collected with *ca.* 72% yield. Elemental analysis Calcd. for $C_{18}H_{19.5}N_4O_{5.75}Cd$(%): C, 43.56; H, 3.96; N, 11.29. Found(%): C, 43.48; H, 4.01; N, 11.23. Selected IR (KBr, cm^{-1}): 3 134(w), 1 647(w), 1 563(w), 1 522(s), 1 493(w), 1 402(s), 1 360(m), 1 280(m), 1 230 (m), 1 128(s), 1 108(s), 1 062(s), 1 028(m), 963(m), 937(s), 861(w), 822(m), 754(s), 689(m).

1.4 Synthesis of {[Zn(ca)(bpe)$_{0.5}$(H_2O)]·H_2O}$_n$ (3)

A starting mixture containing $Zn(OAc)_2·2H_2O$ (21.9 mg, 0.10 mmol), H_2ca (13.0 mg, 0.10 mmol), bpe (18.2 mg, 0.10 mmol), NaOH (4.0 mg, 0.10 mmol) and H_2O (5 mL) was heated at 120 ℃ for 4 days under autogenous pressure, then cooled to room temperature. Colorless sheet crystals of **3** were obtained in 82% yield. Elemental analysis Calcd. for $C_{11}H_{13}NO_6Zn$(%): C, 41.21; H, 4.09; N, 4.37. Found (%): C, 41.18; H, 4.13; N, 4.32. Selected IR (KBr, cm^{-1}): 3 072 (w), 1 655 (w), 1 612(s), 1 562(s), 1 509(s), 1 432(w), 1 401(s), 1 299 (w), 1 262(s), 1 225(m), 1 069(m), 1 065(m), 1 026(s), 985(m), 956(s), 887(m), 872(s), 844(s), 794(m), 726(m).

1.5 Photocatalytic experiments

The photocatalytic activity of complex **3** in degradation of methylene blue (MB) was investigated at ambient temperature under UV light irradiation using a 500 W Xe lamp as light source. The degradation experiments were run as follows: 6 mg complex **3** was added to 6 mL MB (50 μmol·L^{-1}) aqueous solution with 10 μL H_2O_2 (30%) in a glass bottle. The aqueous suspensions were stirred for 30 min in the dark to ensure the adsorption-desorption equilibrium before the light irradiation. During the tracking photocatalytic reaction, the absorbance of 3 mL MB clear solution was measured at 20 min intervals with a UV-Vis spectrophotometer at a 665 nm absorption wavelength, then the solution was poured back into the original suspension. For comparison, the contrast experiment was completed under the same conditions without any catalyst.

1.6 X-ray crystallography

The single-crystal X-ray diffraction analyses were performed on a computer-controlled EosS2 diffractometer equipped with graphite-monochromated Mo $K\alpha$ radiation (λ=0.071 073 nm) by using φ-ω scan technique at room temperature. Using Olex2[19], the structure was solved with the SHELXS[20] program and refined with the SHELXL[21] refinement package. Hydrogen atoms were placed in their geometrically idealized positions and constrained to ride on their parent atoms. The U_{iso} of the H-atoms were constrained to 1.2 times U_{eq} of their bonding carbon atoms with $d_{C\text{-}H}$(aromatic)=0.093 nm and $d_{C\text{-}H}$(methylene)=0.097 nm, and 1.5 times U_{eq} of the hydrogen atoms at water and methyl groups with $d_{C\text{-}H}$(methyl)=0.096 nm. Crystallographic data for complexes **1~3** are listed in Table 1. Selected bond distances and angles and hydrogen bonds are listed in Table S1 and Table S2, respectively.

CCDC: 1913976, **1**; 1913977, **2**; 1913978, **3**.

Table 1　Crystal and structure refinement data for complexes 1~3

Complex	1	2	3
Empirical formula	$C_{18}H_{17}N_4O_{4.75}Zn$	$C_{18}H_{19.5}N_4O_{5.75}Cd$	$C_{11}H_{13}NO_6Zn$
Formula weight	430.72	496.27	320.59
Crystal system	Orthorhombic	Monoclinic	Monoclinic
Space group	*Pbcn*	*C*2/*c*	$P2_1/n$
a / nm	2.164 01(6)	2.019 24(6)	0.795 82(3)
b / nm	1.059 10(3)	1.439 64(5)	1.863 22(8)
c / nm	1.610 72(3)	1.431 29(3)	0.864 82(4)
β / (°)		101.396(3)	96.327(4)

Continued Table 1

V / nm^3	3.691 61(16)	4.078 7(2)	1.274 54(10)
Z	8	8	4
D_c / (g·cm^{-3})	1.550	1.616	1.671
μ / mm^{-1}	1.368	1.111	1.949
F(000)	1 768	1 996	656
θ range for data collection / (°)	3.31 to 25.50	3.39 to 25.50	3.15 to 25.50
Reflection collected, unique	63 865, 3 423	26 249, 3 767	13 970, 2 367
R_{int}	0.059 0	0.025 2	0.043 3
Completeness / %	99.4	99.6	99.7
Data, restraint, parameter	3 423, 103, 278	3 767, 124, 315	2 367, 0, 174
Goodness-of-fit on F^2	1.060	1.104	1.086
R_1, wR_2 [$I>2\sigma(I)$]	0.056 6, 0.141 6	0.037 0, 0.095 4	0.032 4, 0.071 2
R_1, wR_2 (all data)	0.082 3, 0.152 3	0.042 0, 0.098 2	0.038 6, 0.073 9
Largest peak and hole /(e·nm^{-3})	890 and −530	990 and −1 000	310 and −310

2 Results and discussion

2.1 Structure description of {[Zn(ca)(iimb)]·0.75H$_2$O}$_n$ (1)

The complex **1** crystallizes in orthorhombic crystal system, space group *Pbcn* and features a 2D reticular structure. The asymmetric unit contains one crystallographic Zn^{2+}, one ca^{2-}, one iimb molecule, in addition to 0.75 free water molecules. The Zn^{2+} cation adopts a distorted tetrahedral [ZnN_2O_2] coordination environment with two carboxylic oxygen atoms from two symmetry-related ca^{2-} and two nitrogen atoms from two symmetry-related iimb co-ligands (Fig.1a). The Zn-O bond lengths are 0.193 2(10) and 0.196 6(3) nm, and the Zn-N bond lengths are 0.199 9(3) and 0.201 1(3) nm, respectively.

The adjacent Zn^{2+} ions are linked through ca^{2-} adopting the monodentate coordination mode to form a metal-carboxylate chain with the Zn⋯Zn distance of 0.5913 3(1) nm. The adjacent metal-carboxylate chains are further linked by iimb molecules adopting cross connection method along two different directions with the Zn⋯Zn distance of 1.255 41(3) nm to produce two-dimensional network structure (Fig.1b). Each Zn(Ⅱ) ion is connected to four adjacent ones through two ca^{2-} and two iimb co-ligands. The 2D layer can be simplified as a commonly uninodal 4-connected net (Fig.1c). There is no face-face stacking $\pi\cdots\pi$ interaction between the two pyridine and benzene rings of two iimb ligands. The 3D supramolecular structure is formed through weak van der Waals force.

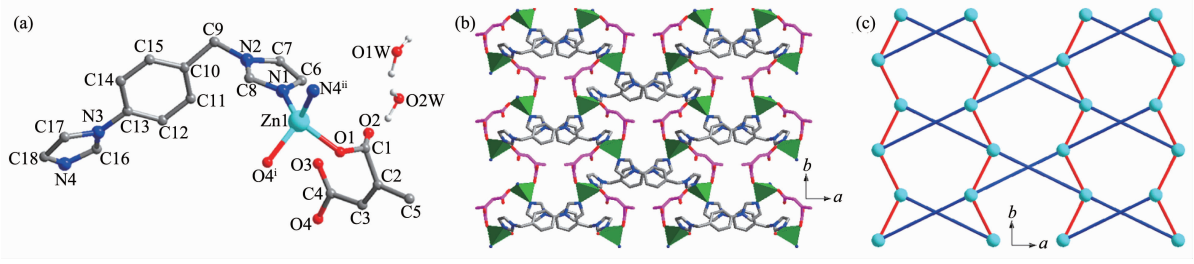

Symmetry codes: [i] 1.5−x, −0.5+y, z; [ii] 0.5+x, −0.5+y, 1.5−z

Fig.1 (a) View of the asymmetric unit showing the local coordination environments of Zn(Ⅱ) in **1**; (b) Polyhedral view of a 2D layer extending in complex **1**; (c) View of schematic representation of 2D layer

2.2 Structure description of {[Cd(ca)(iimb)(H$_2$O)]·0.75H$_2$O}$_n$ (2)

The complex **2** crystallizes in monoclinic crystal system, space group *C*2/*c* and features a one-dimensional double-stranded chain structure. The asymmetric unit contains one crystallographic Cd^{2+}, one ca^{2-}, one iimb

molecule, one coordinated water molecule, in addition to 0.75 free water molecule. The Cd(Ⅱ) ion is coordinated by two nitrogen atoms from two symmetry-related iimb co-ligands, four oxygen atoms from two symmetry-related ca^{2-} and one coordinated water molecule, thus creating a distorted octahedron coordination [Cd(O_4N_2)] geometry (Fig.2a). The Cd-O bond lengths are in a range of 0.230 4(7)~0.266 2(5) nm, and the Cd-N bond lengths are 0.226 1(3) and 0.225 9(3) nm, respectively.

The two carboxylate groups of ca^{2-} adopt the chelating-bidentate and monodentate coordination mode, respectively. Two adjacent Cd(Ⅱ) ions are linked together to form a binuclear cluster with the Cd⋯Cd distance of 0.513 46(1) nm. The carboxylate-bridged dinuclears are extended along the [110] direction by mated iimb co-ligands to produce one 1D coordination polymer with quasi-trapezoidal shape (Fig.2b).

The adjacent chains are linked together by H-bond interactions to form its entire three-dimensional supramolecular structure (Fig.S1). There exist weak inter-chain offset $\pi\cdots\pi$ interactions between benzene ring and imidazole ring of iimb co-ligands, between two parallel benzene rings of iimb co-ligands. The centroids Cg1 (coordinate: −0.044 30, 0.925 04, −0.906 50), Cg3 (coordinate: 0.044 30, 0.925 04, −0.593 50) and Cg4 (coordinate: −0.044 30, 1.074 96, −0.406 50) are made up of atoms including C5, C6, C7, C8, C9 and C10 atoms, moreover, the centroid Cg2 (coordinate: −0.134 23, 1.033 17, 0.703 73) is made up of atoms including N1, C11, N2, C12 and C13 atoms. The centroid-centroid distance (Cg1-Cg2) and the dihedral angle between benzene ring and imidazole ring of iimb co-ligands are 0.402 8 nm and 23.651° respectively. The centroid-centroid distance (Cg3-Cg4) and the dihedral angle between two benzene rings are 0.411 3 nm and 0°, respectively (Fig.S2). It is obvious that the hydrogen bonds and $\pi\cdots\pi$ interactions among the coordination polymers play important roles in the self-assembly and enhanced stability of the resultant structure.

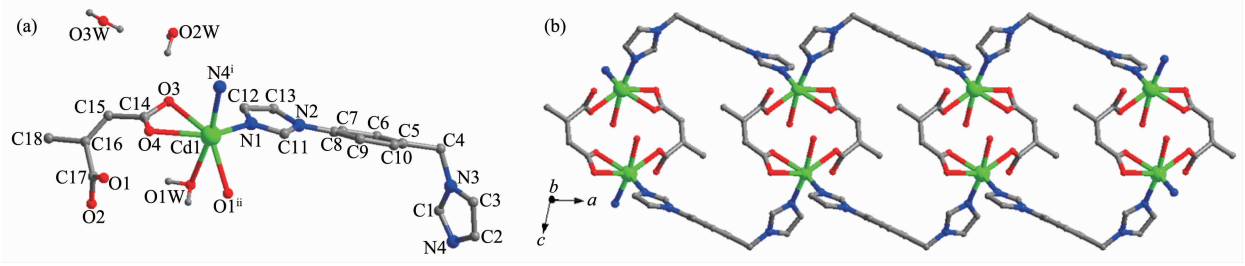

Symmetry codes: [i] −0.5+x, −0.5+y, z; [ii] 0.5−x, 0.5−y, 1−z

Fig.2　(a) View of the asymmetric unit showing the local coordination environments of Cd(Ⅱ) in **2**; (b) Polyhedral view of 1D quasi-trapezoidal shape chain with the dinuclear units

2.3　Structure description of {[Zn(ca)(bpe)$_{0.5}$(H_2O)]·H_2O}$_n$ (3)

The complex **3** crystallizes in monoclinic crystal system, space group $P2_1/n$ and features a two-dimensional wave layer. The asymmetric unit contains one crystallographic Zn^{2+}, one ca^{2-}, half a bpe molecule, one coordinated water and one free water molecule. The Zn^{2+} cation adopts the distorted tetrahedral [$ZnNO_3$] coordination environment with three oxygen atoms from two symmetry-related ca^{2-} and one coordinated water, one nitrogen atom from one bpe co-ligand (Fig.3a). The Zn-O bond lengths are 0.198 11(1), 0.198 79(1) and 0.202 47(1) nm, respectively, and the Zn-N bond length is 0.206 43(1) nm.

The ca^{2-} indeed coordinates to two Zn(Ⅱ) ions from two monodentate sites. The adjacent Zn(Ⅱ) ions are connected by the ca^{2-} to form an interesting corrugated 1D metal-carboxylate chain with the Zn⋯Zn distance of 0.658 09(3) nm (Fig.3b). The neighboring chains are connected by bpe molecules along b direction with the Zn⋯Zn distance of 1.349 50(4) nm to produce a 2D layer (Fig.3c). Each Zn(Ⅱ) ion is connected to three adjacent atoms through two ca^{2-} and one bpe ligand. The 2D layer can be simplified as a commonly

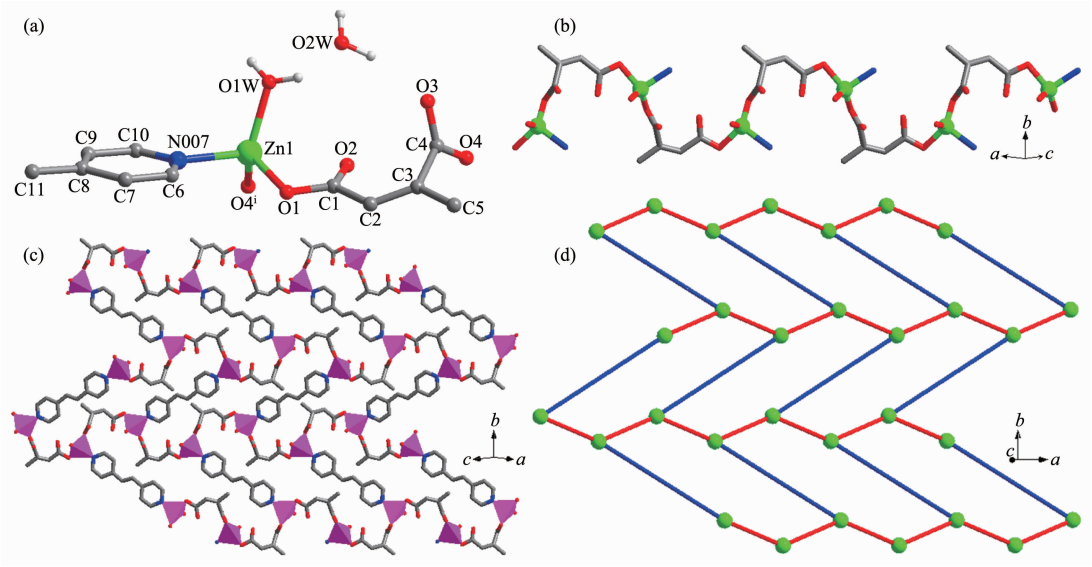

Symmetry codes: [i] $-0.5+x$, $0.5-y$, $0.5+z$

Fig.3 (a) View of the asymmetric unit showing the local coordination environments of Zn(Ⅱ) in **3**; (b) View of a section of the 1D chain by ca^{2-} and Zn^{2+}; (c) Polyhedral view of a 2D wave layer extending in complex **3**; (d) View of schematic representation of 2D layer

uninodal 3-connected grid (Fig.3d).

The adjacent layers are stacked in a -AAA- sequence along special direction to form a three-dimensional supramolecular polymer by interlayer H-bond interactions between the coordinatedwater O atom and the carboxylate O atom of ca^{2-} anions (O(1W)–H(1WA)⋯O(4[i]): O(1W)⋯O(4[i]) 0.271 3(3) nm, ∠O(1W)–H(1WA)⋯O(4[i])=133.2°), between the free water O atom and the carboxylate O atom of ca^{2-} (O(2W)–H(2WA)⋯O(2[ii]): O(2W)⋯O(2[ii]) 0.287 6(3) nm, ∠O(2W)–H(2WA)⋯O(2[ii])= 171.2°, Symmetry codes: [i] $x-1$, y, z; [ii] $x-1/2$, $-y+1/2$, $z-1/2$). There also exist abundant intralayer H-bond interactions between the coordinated water molecule and the guest water molecule (O(1W)–H(1WB)⋯O(2W): O(1W)⋯O(2W) 0.266 6(3) nm, ∠O(1W)–H(1WB)⋯O(2W)=151.4°), between the free water O atom and the carboxylate O atom of ca^{2-} anions (O(2W)–H(2WB)⋯O(3): O(2W)⋯O(3) 0.278 8(3) nm, ∠O(2W)–H(2WB)⋯O(3)=165.5°) (Fig.S3).

2.4 Thermogravimetric analyses and powder X-ray diffraction

The thermogravimetric analyses (TGA) of **1**~**3** were performed on the polycrystalline samples from 25 to 800 ℃ at a heating rate of 10 ℃·min^{-1} under nitrogen atmosphere (Fig.4). The TGA curve of **1** displayed the first weight loss of 3.78% from 60 to 100 ℃ corresponding approximately to release of 0.75 H_2O per formula unit (Calcd. 3.14%). The framework of **1** had a series of weight loss from 260 to 515 ℃ attributed to the decomposition of organic components. The final residue of 10.74% can′t be specifically identified because the theoretical remaining mass of 18.89% is calculated by assuming a final phase ZnO. The TGA curve of **2** displayed 8.59% weight loss in a region of 60~120 ℃, which is not agreement with the calculated value of 1.75 H_2O per formula unit (6.35%), so the 2.24% weight loss corresponds to the water because the sample is not completely dry. Over 250

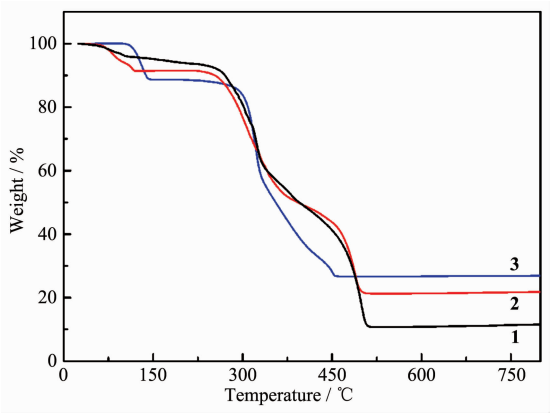

Fig.4 TGA curves for complexes **1**~**3**

℃, the framework of **2** began to gradually decompose until 500 ℃. The final residue of 21.65% can be approximatively identified to final phase CdO because the calculated value of the mass remnant is 25.87%. For **3**, there was no weight loss before 110 ℃, and the first weight loss of 11.16% between 110 and 143 ℃ corresponds to the loss of two water molecules from one coordinated water and one guest water (Calcd. 11.23%). The second weight loss began over 295 ℃ and ended until 454 ℃ corresponding to the decomposition of organic ligands. The observed final mass remnant of 26.63% is almost agreement with the calculated value of the final product ZnO (Calcd. 25.27%). All major peaks in experimental PXRD match quite well that of simulated from the respective single-crystal data, implying their good phase purity (Fig.S4~S6).

2.5 Luminescent properties

The solid-state luminescent properties of three complexes **1**~**3** and free ligands were investigated in the solid state at room temperature, as illustrated in Fig.5. The free H_2ca ligand had no emission peak in a very wide excitation wavelength because of the absence of its conjugation effect. The free bpe and iimb ligands showed fluorescent emission bands at 367 nm (λ_{ex}=334 nm) and 595 nm (λ_{ex}=376 nm). The emission maximums for **1** and **2** occurred at 595 nm upon excitation at a wavelength of 376 nm[9]. The emission spectra of complexes **1** and **2** are completely consistent with that of the powdered free iimb molecule, which should be assigned as the π-π* and/or n-π* transition of the iimb linker. The emission maximum for complex **3** located at 375 nm upon excitation at 280 nm, which displays similar emission spectrum feature to that of the powdered free bpe ligand. The slight red-shift may be attributed to the increase of the ligand conformational rigidity because of the unique coordination of bpe to the Zn(Ⅱ) ion.

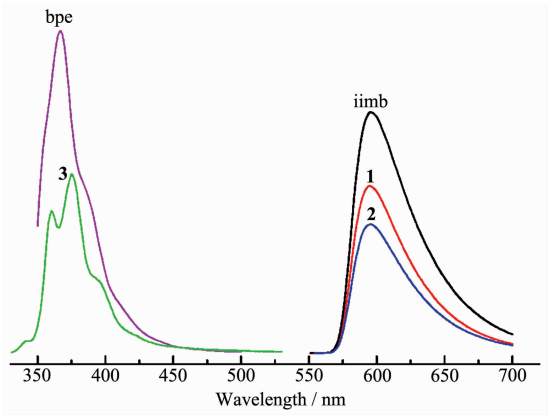

Fig.5　Solid-state emission spectra of complexes **1**~**3** along with the free iimb and bpe ligands

2.6 Photocatalysis property

The organic dyes are one of the largest sources of industrial pollutants. Furthermore, it is difficult to remove organic dyes from industrial wastewater due to their high photo and chemical stability. In recent years, transition metal coordination polymers have been used as a new class of photocatalyst for the decomposition of organic dyes[22-24]. The UV-Vis diffuse reflectance spectrum of complex **3** showed absorption bands at 328 nm, which can be attributed to π-π* transitions of the ligand[25]. The band gap (E_g) derived from Kubelka-Munk function plot is 3.24 eV (Fig.S7). Methylene blue (MB) is one of the largest sources of industrial pollutants. So we chose MB as a representative to investigate the degradation process in detail. There is almost no reduction in concentration of MB with time, and the degradation is almost negligible without H_2O_2 or light irradiation. The photocatalytic behavior of the complex **3** in MB solution is displayed in Fig.6. The organic dye concentrations were estimated by the absorbance at 665 nm (MB). According to Lambert-Beer′s law, the absorbance of a solution is proportional to the concentration of the substance. As shown in Fig.6, approximately 70% of MB was decomposed after 40 min. After 120 min, the photocatalytic efficiency of MB was found to be 97% for **3**. In comparison, the degradation efficiency of MB without any photocatalyst was only about 20% after the same time under the same experimental conditions[26-27]. The apparent rate constant of MB was 0.033 6 min^{-1}, which can be confirmed by the pseudo-first-order reaction model: $\ln(C_t/C_0)=-kt$[28] (Fig.S8), where C_t and C_0 are the concentration of MB at time t and at t=0, and k is the apparent rate constant. To evaluate the stability of photocatalyst **3**, after the photocatalytic process, the complex **3** was recycled by the centrifugation method

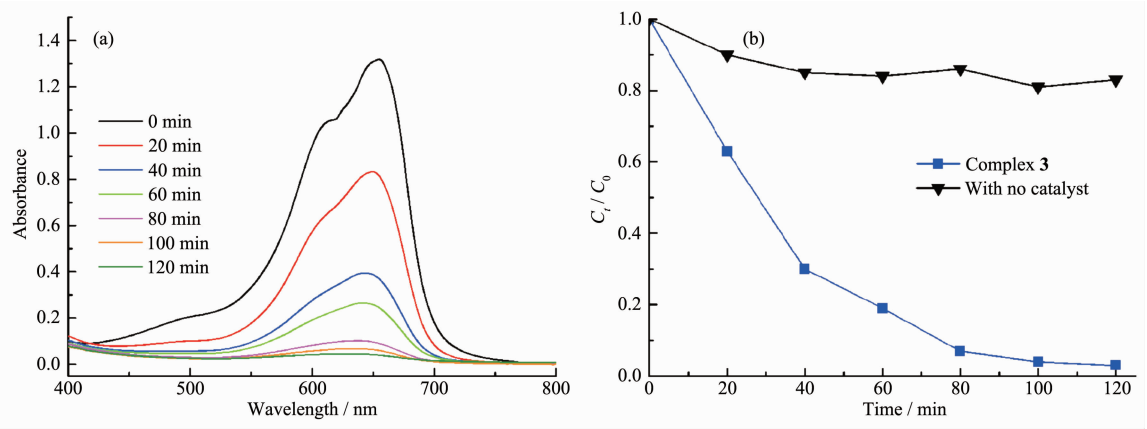

Fig.6 (a) Absorption spectra of the MB solutions during the photodegradation reaction under UV light in the presence of **3**; (b) Concentration changes of MB as a function of irradiation time in the present of **3** and the control experiment without any catalyst

and monitored by powder X-ray diffraction (PXRD) (Fig.S6). The results demonstrated that the complex **3** still maintained a good crystal state after the photocatalytic experiments.

3 Conclusions

In summary, three Zn/Cd(Ⅱ) coordination polymers have been successfully synthesized under hydrothermal conditions. Both complexes **1** and **3** exhibit two dimensional layers containing the metal-carboxylate chains. The complex **2** features a 1D chain structure containing carboxylate-bridged dinuclears. All three complexes show good phase purity and high thermal stability. The emission spectra of three complexes are similar to those of the corresponding N-donor ligands. The photocatalytic experiment result indicates that complex **3** has good photocatalytic activity in decomposing MB in the presence of H_2O_2. The result shows that complex **3** may be a good candidate as photocatalyst with a potential application in wastewater treatment.

Supporting information is available at http://www.wjhxxb.cn

References:

[1] Yu J M, Xie L H, Li J R, et al. *Chem. Rev.*, **2017**,**117**:9674-9754

[2] Zhao Y, Wang L, Fan N N, et al. *Cryst. Growth Des.*, **2018**, **47**:7114-7121

[3] Xin L Y, Liu G Z, Li X L, et al. *Cryst. Growth Des.*, **2012**, **12**:147-157

[4] Zhu L, Liu X Q, Jiang H L, et al. *Chem. Rev.*, **2017**,**117**: 8129-8176

[5] Liu G Z, Li S H, Li X L, et al. *CrystEngComm*, **2013**,**15**: 4571-4580

[6] Xue X, Wang H, Han Y, et al. *Dalton Trans.*, **2018**,**47**:13-22

[7] YIN Wei-Dong(尹卫东), LI Gui-Lian(李桂连), LIU Guang-Zhen(刘广臻), et al. *Chinese J. Inorg. Chem.*(无机化学学报), **2015**,**31**:1439-1446

[8] Naira R M, Sudarsanakumara M R, Sumab S, et al. *J. Mol. Struct.*, **2016**,**1105**:316-321

[9] YIN Wei-Dong(尹卫东), LI Gui-Lian(李桂连), LI Xiao-Ling(李晓玲), et al. *Chinese J. Inorg. Chem.*(无机化学学报), **2016**,**32**:662-668

[10]Yin W D, Shen J, He Y Y, et al. *Transition Met. Chem.*, **2019**,**44**:89-97

[11]Xu X X, Zhang X, Liu X X, et al. *Cryst. Growth Des.*, **2010**, **10**:2272-2277

[12]Di Nicola C, Forlin E, Garau F, et al. *J. Organomet. Chem.*, **2012**,**714**:74-80

[13]Yin W D, Li G L, Xin L Y, et al. *Chin. J. Struct. Chem.*, **2017**,**36**:1502-1510

[14]WANG Yu-Fang(王玉芳), TAI Jun-Hui(太军慧), YAN Xiao-Wei(颜小伟), et al. *Chinese J. Inorg. Chem.*(无机化学学报), **2018**,**34**:1121-1126

[15]Liu G Z, Xin L Y, Wang L Y. *CrystEngComm*, **2011**,**13**: 3013-3020

[16]Li X L, Liu G Z, Xin L Y, et al. *CrystEngComm*, **2012**,**14**: 1729-1736

[17]Xin L Y, Liu G Z, Ma L F, et al. *J. Solid State Chem.*, **2013**, **206**:233-241

[18]Li Z H, Xue L P, Qin Q P, et al. *J. Solid State Chem.*, **2019**, **274**:81-85

[19]Dolomanov O V, Bourhis L J, Gildea R J, et al. *J. Appl. Cryst.*, **2009**,**42**:339-341

[20]Sheldrick G M. *Acta Crystallogr. Sect. A*: *Found. Crystallogr.*, **2015**,**A71**:3-8

[21]Sheldrick G M. *Acta Crystallogr. Sect. C*: *Cryst. Struct. Commun.*, **2015**,**C71**:3-8

[22]LIU Yuan-Yuan(刘媛媛), ZHANG Hui-Min(张慧敏), WANG Xin-Rui(王鑫蕊), et al. *Chinese J. Inorg. Chem.*(无机化学学报), **2018**,**34**:791-799

[23]Qin L, Chen H Z, Lei J, et al. *Cryst. Growth Des.*, **2017**,**17**: 1293-1298

[24]Wang C, Xing F, Bai Y L, et al. *Cryst. Growth Des.*, **2016**, **16**:2277-2288

[25]Hao S Y, Hou S X, Van Hecke K, et al. *Dalton Trans.*, **2017**, **46**:1951-1964

[26]Guo J, Ma J F, Li J J, et al. *Cryst. Growth Des.*, **2012**,**12**: 6074-6082

[27]Wang Z H, Hao R, Zhu S, et al. *Chin. J. Struct. Chem.*, **2018**,**37**:803-810

[28]ZHAI Li-Jun(翟丽军), NIU Yu-Lan(牛宇岚), HAO Xiao-Yan(郝小艳), et al. *Chinese J. Inorg. Chem.*(无机化学学报), **2018**,**34**:1936-1942